Experimental and theoretical study of electron momentum density of K_6C_{60} and comparison to pristine C_{60}

M. Marangolo

Laboratoire de Minéralogie-Cristallographie de Paris, Université Paris VI, case 115, 4 place Jussieu, 75252 Paris Cedex 05, France

J. Moscovici*

Groupe de Physique des Milieux Denses, Université Paris XII, 61 avenue G1 de Gaulle, 94010, Creteil Cedex, France

G. Loupias*

Laboratoire de Minéralogie-Cristallographie de Paris, Université Paris VI, case 115, 4 place Jussieu, 75252 Paris Cedex 05, France

S. Rabii

Department of Electrical Engineering, University of Pennsylvania, Philadelphia, Pennsylvania 19104-6390

S. C. Erwin

Complex Systems Theory Branch, NRL, Washington, D.C. 20375

C. Hérold, J. F. Marêché, and Ph. Lagrange

Laboratoire de Chimie du Solide Minéral, Université Nancy I, Boîte Postale 239, 54506 Vandoeuvre-Cedex, France

(Received 15 April 1998)

Compton profile measurements on K_6C_{60} and C_{60} powders have been carried out using inelastically scattered 16-keV photons. Experimental results are compared with profiles obtained from *ab initio* self-consistent-field calculations of the energy band structure. The good agreement between experimental and theoretical results allows us to discuss the weakening of bonds due to a little but measurable electron density distortion on the C_{60} molecule after potassium intercalation. [S0163-1829(98)00636-5]

I. INTRODUCTION

The intercalation of fullerenes with heavy alkali atoms (K, Rb, and Cs) leads to a series of compounds M_nC_{60} (n ranging from 0 to 6) with important modifications of structural and electronic properties of the host material.[1–3] The compounds M_6C_{60} are of particular interest for understanding the nature of bonding in these compounds. Unlike C_{60} itself, they are orientationally ordered,[4] making them particularly suitable for theoretical investigations.[5,6]

In this paper we report on a combined experimental and theoretical momentum-space study of the two end compounds in this series. The experimental approach utilizes the inelastic scattering of x rays to obtain Compton profiles (CP's) of K_6C_{60} and C_{60}. This technique, which is a bulk probe, is particularly suitable for the investigation of synthetic materials since due to its incoherence it is not sensitive to defects in the sample. Furthermore, it is particularly sensitive to valence electrons, which play a major role in determining the structural and electronic properties of solids. Our aim is to evaluate the valence electron density after the intercalation of pristine C_{60} in order to study the resulting the molecular distortion of the C_{60} cage. We have already demonstrated the utility of this approach in the case of alkaligraphite intercalation compounds, which are two-dimensional analogs of the M_xC_{60} family.[7–12]

Compton scattering probes the ground-state electron momentum density, which in turn can be related to the plane-wave expansion of the ground-state wave functions. Thus experimental profiles can also be used to evaluate the quality of the calculated wave functions.

In Sec. II we introduce Compton scattering. Section III describes the theoretical approach. The experimental procedures, including sample preparation and characterization, are presented in Sec. IV. Results and conclusions are given in Sec. V.

II. COMPTON SCATTERING METHOD

Compton scattering involves the inelastic scattering of photons by electrons. Conservation of energy and momentum leads to the following relationship for the wavelength shift of photons, as a result of the scattering process:

$$\Delta\lambda = \frac{2h}{mc}\sin^2\left(\frac{\varphi}{2}\right) + \frac{2\lambda_1}{mc}\sin\left(\frac{\varphi}{2}\right)q, \tag{1}$$

where φ is the scattering angle, λ_1 is the incoming beam wavelength, and q is the value of the electron momentum in the scattering direction.

The wavelength shift of the photons is composed of two terms.[13] The first term is due to the scattering of a photon by an electron at rest and is referred to as the Compton shift. The second contribution is due to Doppler broadening around the Compton shift, resulting from the motion of the electron in the solid.[14,15] Within the impulse approximation, the directional Compton profile is defined as

$$J(q,\mathbf{e}) = \int n(\mathbf{p})\,\delta(\mathbf{p}\cdot\mathbf{e})d\mathbf{p} = \int \chi^*(\mathbf{p})\chi(\mathbf{p})\,\delta(\mathbf{p}\cdot\mathbf{e}-q)d\mathbf{p}, \tag{2}$$
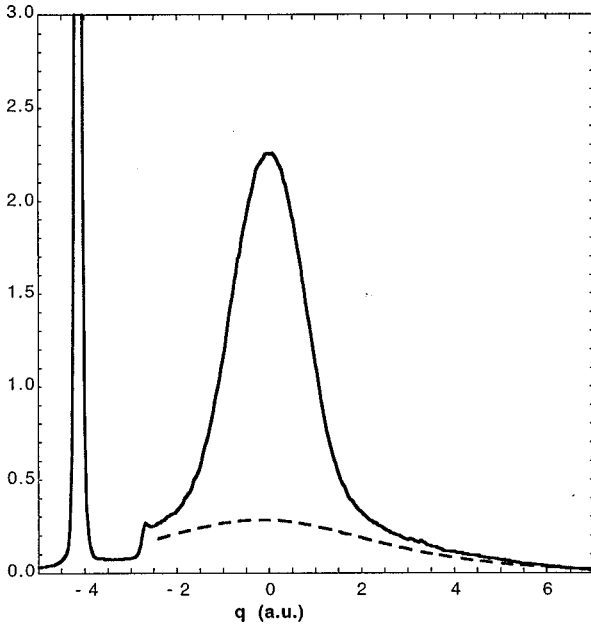
FIG. 1. Total experimental Compton profile of C_{60} (solid line) and the QSCF core profile (dashed line). The measurements were made with $E_1 = 16.4$ keV photons with a scattering angle $\Phi = 135°$. There is a noticeable Raman departure at $q = -2.8$ a.u.

where $\mathbf{e}$ is the unit vector along the scattering vector $\mathbf{K}$, $n(\mathbf{p})$ is the electron momentum density, and $\chi(\mathbf{p})$ is the wave function of the electron in momentum space, i.e., the Fourier transform of the wave function in real space.[15,16] Throughout the remainder of this paper we shall use atomic units (a.u.), for which $\hbar = m = 1$.

Figure 1 shows the measured profile of C_{60}. Due to the flatness of the core electron profile in momentum space, it is easy to subtract its contribution from the measured total profile, resulting in the profile due to the valence electrons alone. The carbon $1s$ core profile is also shown in Fig. 1. It is possible to notice the fine structure at $q = -2.8$ a.u. (Raman departure), which is related to the empty states in solid C_{60}.

III. THEORETICAL APPROACH

The electronic structure of C_{60} (Ref. 2) and K_6C_{60} (Ref. 5) were calculated within the local-density approximation using the Ceperly-Adler exchange-correlation functional. The Kohn-Sham equations were solved using the *ab initio* linear combination of atomic orbitals method. The localized orbitals were expanded on a set of Gaussian-orbital basis functions. The basis set for carbon included $4s$-type and $3p$-type Gaussian functions, while for potassium it contained five s-type and four p-type functions. The calculations were self-consistent, with no restrictions on the form of charge density or potential. Due to the large size of the unit cell, a single k point (Γ) was sufficient to achieve convergence in the Brillouin zone (BZ) integration. The details of the formalism are given in Ref. 17.

The ground-state wave functions were then expanded in plane waves to be used in the calculations of directional Compton profiles. If the wave functions are represented by their plane-wave expansion

$$\psi_{n,\mathbf{k}}(\mathbf{r}) = \sum_{\mathbf{G}} C_{n,\mathbf{k}}(\mathbf{G}) \exp[i(\mathbf{k}+\mathbf{G})\cdot\mathbf{r}], \qquad (3)$$

where $\mathbf{G}$'s are reciprocal lattice vectors, the directional Compton profile can be written as[11]

$$J(q,\mathbf{e}) = \frac{1}{N} \sum_n \sum_{\mathbf{k}} \sum_{\mathbf{G}} |C_{n,\mathbf{k}}(\mathbf{G})|^2$$
$$\times \delta((\mathbf{k}+\mathbf{G})\cdot\mathbf{e}-\mathbf{q})\,\vartheta(E_n-E_f). \qquad (4)$$

The summation $\mathbf{G}$ is over all the reciprocal lattice vectors for which the $C_{n,\mathbf{k}}(\mathbf{G})$'s are non-negligible. The number of $\mathbf{G}$'s required to achieve convergence is related to the size of the primitive unit cell. In our experience, it has ranged from 2000 to 64 000 vectors, respectively, for graphite and fullerenes, reflecting the vastly different lengths for the reciprocal lattice basis vectors. For C_{60} and K_6C_{60} this number was chosen as 64 000. Summation $\mathbf{k}$ is over the symmetry-reduced sector of the BZ, using a tetrahedral interpolation method.[18] The volume of this irreducible sector of the BZ is divided into tetrahedra by choosing a grid of $\mathbf{k}$ points. The actual wave functions are calculated at each grid point and a linear interpolation is carried out for $|C_{n,k}(G)|^2$ within each tetrahedron. Due to the small volume of the BZ for these compounds, a relatively coarse mesh is sufficient for the BZ integration, 11 $\mathbf{k}$ points for C_{60} and 14 for K_6C_{60}. The summation n is over the occupied states. The function ϑ cuts off this summation at Fermi energy in the case where the material is a metal or a semimetal. In this case we are dealing with insulators, which makes this cutoff unnecessary. Since the measurements are performed on powder samples, the comparison is made with the average theoretical profile obtained by four directional profiles.

IV. EXPERIMENTAL PROCEDURE

A. Sample preparation and characterization

C_{60} powder from Hoechst company is used in this study. Before its intercalation, the powder that contains some impurities, in particular sulfur, is meticulously purified. This purification consists of a very slow outgassing under high vacuum, from room temperature to 400 °C. The temperature is progressively increased, so that the pressure remains lower than 10^{-5} mm Hg. The process takes 4–6 weeks. An x-ray absorption near-edge structure study was used to show that this treatment has removed all impurities, even oxygen, completely.[19] After outgassing, the powder is transferred under a pure argon atmosphere to avoid new oxygen contamination.

The saturated K_6C_{60} compound is prepared by reaction of an excess amount of alkali metal and a weighted quantity of C_{60} powder (200 mg). The reaction is carried out in a vacuum sealed Pyrex glass tube at 200 °C for 3 weeks. A gradient of a few degrees is maintained along the tube to prevent metal from condensing onto C_{60}. The powder is then put in a Lindemann capillary under a pure argon atmosphere for x-ray examination. The x-ray powder diffraction pattern collected with Mo $K\alpha_1$ radiation show clearly that all reflections can be indexed on a body-centered-cubic lattice with a parameter of $a = 11.39$ Å.[4]

B. Experimental setup

The experiments were carried out using the high-resolution spectrometer of the high-energy synchrotron at Laboratoire d'Utilisation du Rayonnement Electromagnétique in Orsay, France.[20] The positron storage ring operates at 1.85 GeV and a three-pole superconductor magnet wiggler provides a beam with a critical energy of about 8 keV. The synchrotron radiation beam is monochromatized by Bragg reflection from a double (220) silicon monochromator to produce an energy of 16 363 eV.[21] The beam is sagittally focused on the powder sample of K_6C_{60} by the monochromator's second crystal. The sample is a cylinder of 5 mm height and 6 mm diameter. The powder was kept under dry argon atmosphere at all times.

A high-resolution focusing spectrometer is used to energy analyze the photons scattered by the sample at an angle of 135°. The Cauchois analyzing crystal is made of curved silicon, asymmetrically cut to employ the (620) reflection. Photons of the same energy are focused at a single point on the Rowland circle and detected by a position-sensitive detector, filled with xenon at 4 atm. The whole spectrum is collected at the same time. The entire path of this scattered beam is maintained under vacuum.

The resolution function is deduced from the full width at half maximum of the thermal diffuse scattering peak, which was 0.15 a.u. of momentum. The separation between the experimental data points is equivalent to 0.03 a.u. when expressed in terms of the momentum scale. At the Compton peak 3×10^6 counts were collected. For the purpose of a comparison, the Compton profile of C_{60} powder was also measured exactly under the same experimental conditions, with 2×10^6 counts at the Compton peak.

C. Data processing

After subtracting the background, the raw data were corrected for wavelength-dependent terms such as absorption (in the sample and analyzer), detector efficiency, and analyzer reflectivity predicted by kinematic theory.[22] The wavelength scale was then converted into a momentum scale. The contribution due to multiply scattered photons was subtracted from the measured profile in order to obtain the total Compton profile. These multiple-scattering contributions were calculated using a Monte Carlo simulation and taking into account beam polarization, sample geometry, and density.[23] The ratio of the double scattering to the total was 3% in the case of K_6C_{60} and 5% in the case of C_{60}. The triple scattering was negligibly small.

In order to obtain the profile due to the valence electrons alone, the core electron profiles were subtracted from the total measured profile. Under the impulse approximation, the core contribution is obtained from atomic wave functions.[24] This approximation is valid only if the energy ΔE transferred from the photon to the ejected electron is large compared to the binding energy of the electron.[13]

In our case, considering the Compton shift of 842 eV, compared to binding energies of potassium $2s$ and carbon $1s$ ranging between 200 and 300 eV, it was necessary to move beyond the impulse approximation and use the quasi-self-
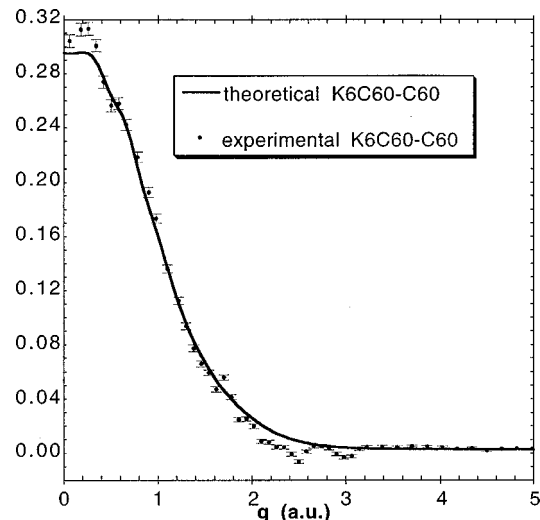

FIG. 2. Differences between the valence Compton profiles of K_6C_{60} and C_{60}. These profiles are affected by the contribution of K $3p$ electrons.

consistent-field (QSCF) method to obtain the core profiles for the C $1s$ and K $1s$ (Raman departure at 14.4 a.u.), $2s$, $2p$, and $3s$ electrons.[24]

The potassium $3p$ core electrons will be treated as "pseudocore" as described in the next section. After removing the core and pseudocore contributions, the remaining profile is normalized to the number of valence electrons per carbon atom, i.e., 4.10 in K_6C_{60} and 4 in C_{60}.

V. RESULTS AND DISCUSSION

In Fig. 2 we show a comparison between theory and experiment for the Compton profile of K_6C_{60} minus that of C_{60}. These difference profiles include the contribution of K $3p$ electrons; therefore, the area under the curves corresponds to 0.7 electron for the full profile. Profile differences eliminate systematic errors, including the neglect of electron-electron correlation effects on the calculated wave functions.[25] The overall agreement between theory and experiment is very good.

In Fig. 3 we show the band structure of K_6C_{60} down to 25 eV, where K $3p$ states form a complex isolated from the narrower carbon bands. The bandlike nature of these states, which is due to K-K "indirect hopping," is clearly apparent. Photoemission spectroscopy[26] has already demonstrated that K $3p$ emission has a bandlike character and, in addition, has suggested that K $3p$ wave functions in K_3C_{60} as in K_6C_{60} are extended enough to overlap with orbitals of surrounding fullerenes. Our calculations indicate that the K $3p$ admixture in filled carbon-type bands is less than 4%.

In order to be able to compare K_6C_{60} and C_{60} in a meaningful manner, it is necessary to subtract out the K $3p$ contribution from both the calculated and measured profiles in K_6C_{60}. This is rather simple in the case of the calculated profiles due to the aforementioned isolation of these bands, allowing us to obtain the theoretical K $3p$ profile, i.e., the pseudocore. We subtract this contribution from both the calculated and measured profiles. In order to observe the characteristics of the additional electrons in the solid after the
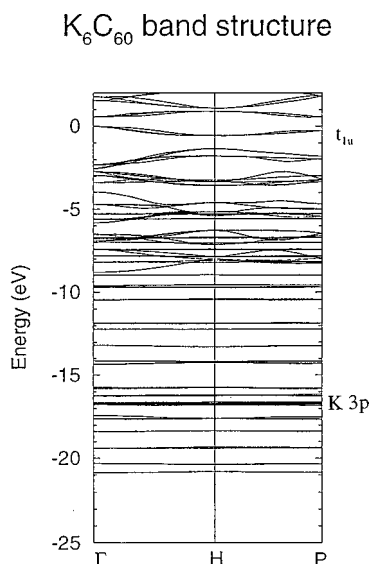
K_6C_{60} band structure

FIG. 3. Self-consistent electronic energy band structure of crystalline K_6C_{60}. The energy zero is set to the valence-band maximum. K $3p$ bands are marked.

potassium intercalation, as well as the modifications in pristine C_{60} electronic distribution brought about by intercalation, we show the difference between profiles of K_6C_{60} and C_{60},[27] after core and pseudocore subtraction (Fig. 4) in both theory and experiment. We stress that this Compton profile difference (CPD) is due to two contributions.

The first contribution is due to the electrons in the upper complex of three bands (Fig. 3) originating from the molecular t_{1u} lowest unoccupied molecular orbital levels in C_{60}. This complex forms the conduction band in K_nC_{60}, which becomes completely filled for $n=6$. We call this contribution the conduction profile. The second contribution that is related to the distortion of the pristine C_{60} electronic density is due the to the presence of the K^+ ions, which we call the distortion profile.

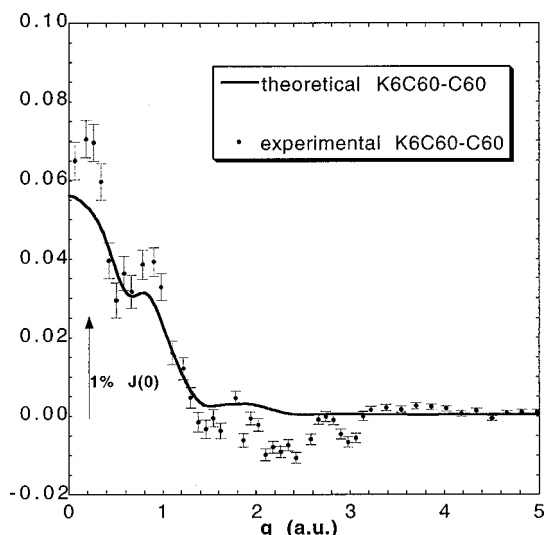While neither of these two quantities is accessible experi-

FIG. 4. Differences between valence Compton profiles of K_6C_{60} and C_{60}. The potassium $3p$ bandlike contribution to the CP has been subtracted.
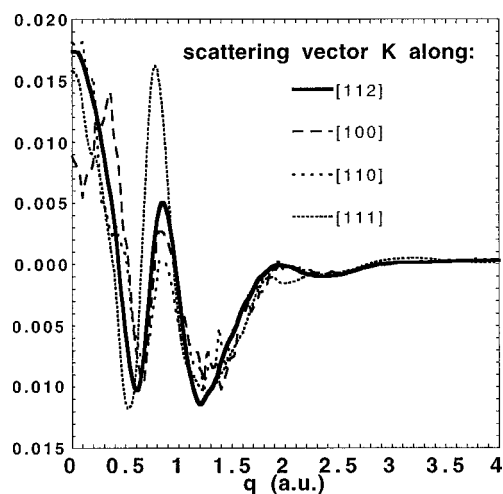

FIG. 5. Calculated distortion of directional profiles. These profiles are related to the distortion of the filled orbitals of C_{60} due to the presence of the potassium ions, so the net area under this profile is zero.

mentally, their sum is simply the difference between the total profiles of K_6C_{60} and C_{60}, excluding the core and pseudocore contributions (Fig. 4). In order to investigate these two effects we have separately calculated their contributions to the CPD. Figure 5 shows the directional distortion profiles for four directions. Since this simply represents the distortion of the filled orbitals of C_{60} due to the presence of the potassium ions, the net area under this profile is zero. This general behavior is similar for all the calculated directional profiles. The other contribution, i.e., the conduction profile, is due to the electrons occupying the filled t_{1u} band in K_6C_{60} (Fig. 6). Local-density approximation calculations[17] suggest strongly that bonding in crystalline K_6C_{60} is almost entirely ionic: The charge-transfer reaction $C_{60}+6K \rightarrow C_{60}^6+6K^{+1}$ is energetically favorable. The $4s$ K electrons, transferred to the t_{1u} C_{60} bands, lead to the calculated conduction profile of K_6C_{60}. Nothing needs to be subtracted from this contribution due to the fact that these bands are empty in pristine C_{60}. The area
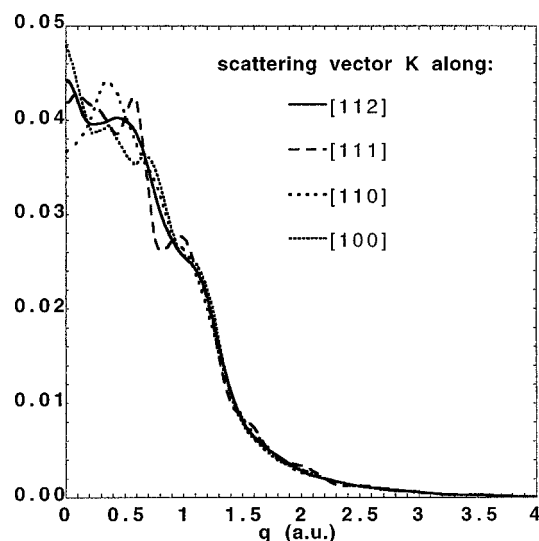

FIG. 6. Calculated conduction profile due to the electrons occupying the t_{1u} conduction band in K_6C_{60}.
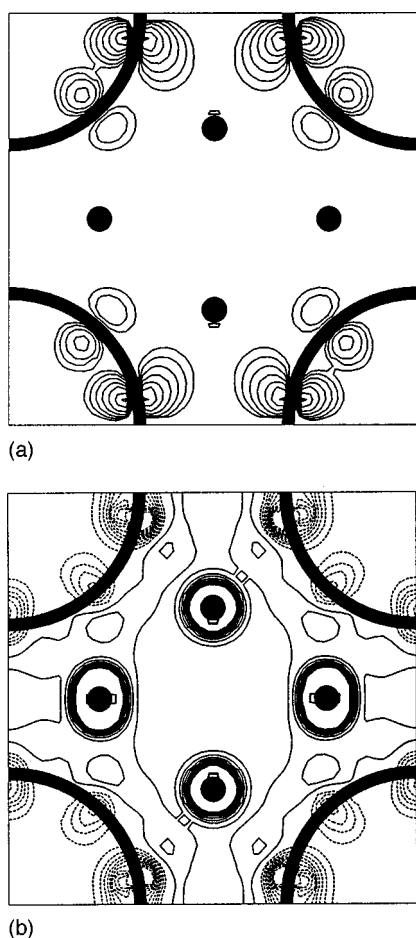
(a)

(b)

FIG. 7. (a) t_{1u} bands density contour plot in the (100) plane. The contours are logarithmically spaced (adjacent contours differ by a factor 2). The minimum contour density is 2×10^{-11} electrons/bohr^3. (b) Difference charge-density contour in the (100) plane obtained by subtracting the charge density of a hypothetical bcc C_{60} solid from the ''valence'' charge density of K_6C_{60}. The contours are linearly spaced from -0.01 to 0.01 electrons/bohr^3: dashed, negative; solid, positive.

of this contribution is equal to 0.1 electron, i.e., the extra charge on each carbon atom. The conduction profile, always positive, is close to zero at $q = 3$ a.u.. Figure 7(a) shows the charge-density contours in the (100) plane. We recognize the mainly π^* character of these orbitals.

We also see the strong π character of these orbitals, in momentum space, by observing the calculated conduction profile. It is well known that π orbitals that are parallel to the scattering vector lead to a Compton profile that is zero at $q = 0$ and have a nonzero momentum maximum in the region of $q = 1$ a.u.[28] In contrast, π orbitals that are perpendicular to the scattering vector lead to a Compton profile whose maximum is at $q = 0$, without any structure in the region of $q = 1$ a.u. Since C_{60} molecules are almost spherical, some of the π^* orbitals will be parallel, some perpendicular, and

some intermediate with respect to the scattering vector. The observed shoulder near $q = 1$ a.u. is due to π orbitals parallel to the scattering vector.

The distortion profile (Fig. 5) is positive at low q (denoting electron delocalization), zero for q larger than 3 a.u., and shows a structure around $q = 0.8$ a.u. The $q = 0.8$ structure can be described by the shift of the maximum of the CP of 1 a.u. derived from the mainly π character orbitals (parallel to the scattering vector), towards lower q values, i.e., an effect of the electronic delocalization in K_6C_{60} compared to C_{60}.

This trend is similar for all the calculated directional CPD's. The contribution of these marked and narrow profiles to the CPD is 2–3 times lower than the order of magnitude of the filled conduction-band Compton profile (Fig. 6). In order to clarify the main features of this calculated distortion profile, in Fig. 7(b) we show the difference charge-density contours. These contours are obtained by subtracting the charge density of a hypothetical C_{60} solid with a bcc structure and the same lattice constant as for K_6C_{60}, from the ''valence'' charge density of K_6C_{60}. The contours are again in the (100) plane. The plot suggests that the main effect of the potassium intercalation in K_6C_{60} is to draw charge out of the C-C bonds of each molecule to further delocalize the electron density. It has already been shown that K ions weaken some of the bonds in a C_{60} molecule and this charge is partly on the face of C_{60} hexagons and partly forming small dangling-bond-like structures on all six C atoms, in the direction perpendicular to the C-C bonds.[17]

The good agreement between calculated and experimental CPD's corroborates the scenario of a small but measurable delocalization of the valence electron density due to the intercalation of K ions. It is important to point out that such an effect actually corresponds to a very small distortion of the pristine C_{60} orbitals.

Although there is good overall agreement between theory and experience in Fig. 4, we notice that the experimental CPD is negative in the range 2 a.u.$< q <$3 a.u.: This phenomenon is not seen in the calculated CPD. A small underestimation of the delocalization of carbon bonds could be the cause of this discrepancy.

In conclusion, our combined experimental and theoretical study of momentum density in K_6C_{60} and C_{60} indicates that intercalation with K leads to a nonrigid transfer of charge from K to the previously unoccupied t_{1u} bands of C_{60}. The presence of K^+ ions leads to a small but clearly observable distortion of the charge density of C_{60} molecules in K_6C_{60} and to an overall delocalization of charge away from the C-C bonds.

*Also at Laboratoire pour l'Utilisation du Rayonnement Electromagnetique, Bâtiment 209, Université Paris-Sud, 91405 Orsay Cedex, France.

[1] K. Prassides and H. Kroto, Phys. World **44**, 35 (1992).

[2] S. C. Erwin, in *Buckminsterfullerenes*, edited by W. E. Billups and M. A. Ciufolini (VCH, New York, 1993), p. 217.

[3] P. J. Benning, F. Stepniak, D. M. Poirier, J. L. Martins, J. H. Weaver, L. P. F. Chiabante, and R. E. Smalley, Phys. Rev. B **47**,

13 843 (1993).

[4] O. Zhou, J. E. Fischer, N. Coustel, S. Kycia, Q. Zhu, A. R. McGhie, W. J. Romanow, J. P. McCauley, A. B. Smith, and D. E. Cox, Nature (London) **351**, 462 (1991).

[5] S. C. Erwin and M. R. Pederson, Phys. Rev. Lett. **67**, 1610 (1991).

[6] M. Huang, Y. Xu, and W. Y. Ching, J. Chem. Phys. **96**, 1648 (1992); J. L. Martins and N. Troullier, Phys. Rev. B **46**, 1766 (1992); W. Andreoni, F. Gygi, and M. Parrinello, Phys. Rev. Lett. **68**, 823 (1992); W. Andreoni, P. Giannozzi, and M. Parrinello, Phys. Rev. B **51**, 2087 (1995).

[7] G. Loupias, J. Chomilier, and D. Guérard, J. Phys. (France) Lett. **45**, L301 (1984).

[8] M. Y. Chou, S. Louie, M. L. Cohen, and N. Holzwarth, Phys. Rev. B **30**, 1062 (1984).

[9] G. Loupias, J. Chomilier, and D. Guérard, Solid State Commun. **55**, 299 (1985).

[10] M. Y. Chou, M. L. Cohen, and S. G. Louie, Phys. Rev. B **33**, 6619 (1986).

[11] S. Rabii, J. Chomilier, and G. Loupias, Phys. Rev. B **40**, 10 105 (1989).

[12] G. Loupias, R. Wentzcovitch, L. Bellaïche, J. Moscovici, and S. Rabii, Phys. Rev. B **49**, 13 342 (1994).

[13] J. W. M. DuMond, Phys. Rev. **33**, 643 (1929); **36**, 146 (1930).

[14] P. Eisenberger and P. M. Platzman, Phys. Rev. A **2**, 415 (1970).

[15] M. J. Cooper, Rep. Prog. Phys. **48**, 415 (1985).

[16] L. Mendelsohn and V. H. Smith, in *Compton Scattering*, edited by Brian Williams (McGraw-Hill, New York, 1977).

[17] S. C. Erwin, M. R. Pederson, and W. E. Pickett, Phys. Rev. B **41**, 10 437 (1992).

[18] G. Lehmann and M. Taut, Phys. Status Solidi B **87**, 221 (1978).

[19] P. Lagrange, D. Bégin, C. Hérold, and J. F. Marêché (unpublished).

[20] G. Loupias, J. Petiau, A. Issolah, and M. Schneider, Phys. Status Solidi B **102**, 79 (1980).

[21] J. Frouin, Y. Garreau, G. Loupias, D. Raoux, and J. Tarbès, Nucl. Instrum. Methods Phys. Res. A **266**, 484 (1988).

[22] F. Balibar, Y. Epelboin, and C. Malgrange, Acta Crystallogr., Sect. A: Cryst. Phys., Diffr., Theor. Gen. Crystallogr. **31**, 836 (1975).

[23] J. Chomilier, G. Loupias, and J. Felsteiner, Nucl. Instrum. Methods Phys. Res. A **235**, 603 (1985).

[24] A. Issolah, B. Lévy, A. Beswick, and G. Loupias, Phys. Rev. A **38**, 4509 (1988); A. Issolah, Y. Garreau, B. Lévy, and G. Loupias, Phys. Rev. B **44**, 11 029 (1991).

[25] P. Rennert, Phys. Status Solidi B **105**, 567 (1981); M. L. Chou, P. K. Lam, M. L. Cohen, G. Loupias, J. Chomilier, and J. Petiau, Phys. Rev. Lett. **49**, 1452 (1982).

[26] P. J. Benning, D. M. Poirier, T. R. Ohno, Y. Chen, M. B. Jost, F. Stepniak, G. H. Kroll, J. H. Weaver, J. Fure, and R. E. Smalley, Phys. Rev. B **45**, 6899 (1992).

[27] J. Moscovici, G. Loupias, S. Rabii, S. Erwin, A. Rassat, and C. Fabre, Europhys. Lett. **31**, 87 (1995).

[28] M. J. Cooper and J. A. Leake, Philos. Mag. **15**, 1201 (1967).